J. Fluid Mech. (2005), *vol.* 536, *pp.* 367–376.
doi:10.1017/S0022112005005264 Printed in the United Kingdom

Buoyancy flux bounds for surface-driven flow

By C. P. CAULFIELD

Department of Mechanical and Aerospace Engineering, Jacobs School of Engineering, University of California, San Diego, 9500 Gilman Drive, La Jolla, CA 92093-0411, USA

(Received 5 April 2005 and in revised form 11 May 2005)

I calculate the optimal upper bound, subject to the assumption of streamwise invariance, on the long-time-averaged buoyancy flux $\mathscr{B}^*$ within the flow of an incompressible stratified viscous fluid of constant kinematic viscosity ν and depth h driven by a constant surface stress $\tau = \rho u_\star^2$, where $u_\star$ is the friction velocity with a constant statically stable density difference $\Delta\rho$ maintained across the layer. By using the variational 'background method' (due to Constantin, Doering and Hopf) and numerical continuation, I generate a rigorous upper bound on the buoyancy flux for arbitrary Grashof numbers G, where $G = \tau h^2/(\rho\nu^2)$. As $G \to \infty$, for flows where horizontal mean momentum balance, horizontally averaged heat balance, total power balance and total entropy flux balance are imposed as constraints, I show numerically that the best possible upper bound for the buoyancy flux is given by $\mathscr{B}^* \leqslant \mathscr{B}^*_{\max} = u_\star^4/(4\nu) + O(u_\star^3/h)$. This bound is independent of both the overall strength of the stratification and the layer depth to leading order. This bound is associated with a velocity profile that has the scaling characteristics of a somewhat decelerated laminar, linear velocity profile.

1. Introduction

In stratified geophysical flows, such as occur in the atmosphere and ocean, it is critically important to understand how external forcing mechanisms drive the flow, trigger and sustain turbulence, and modify irreversibly (i.e. 'mix') the density distribution within the flow. Such an understanding is essential to the development of accurate parameterizations within larger-scale models of mixing processes, which have a qualitative impact on the time evolution of the flow. One particular issue of interest to parameterizations is the question of whether it is possible to identify bounds on mixing, dependent potentially on various parameters which characterize the flow behaviour. Naturally, it is to be expected that the properties of the mixing are strongly dependent on the particular form of the flow forcing mechanisms (typically associated with vertical velocity shear) and so it is also necessary to consider a range of realistic forcing mechanisms to build up a general and useful picture of the properties of bounds on mixing within stratified flows.

A valuable tool for the identification of such bounds is the so-called CDH method, (following Plasting & Kerswell 2003, henceforth referred to as PK03) due to Constantin and Doering (see Doering & Constantin 1992). This method relies on a particular insight of Hopf (1941) and was subsequently improved by Nicodemus, Holthaus & Grossmann (1997). The method uses a non-unique decomposition of the flow fields into steady 'background' fields that satisfy the inhomogeneous boundary conditions, and 'fluctuations' away from these backgrounds which satisfy homogeneous boundary conditions. As discussed in more detail below, these background

fields also may act (within a variational problem) as Lagrange multipliers, imposing constraints related to horizontal averages of the flow governing equations. Conventional techniques of the calculus of variations and numerical continuation may then be used to generate bounds on quadratic flow quantities of interest, such as the long-time average of the mechanical energy dissipation rate (see e.g. PK03) or the long-time average of the buoyancy flux (see Caulfield, Tang & Plasting 2004, henceforth CTP04).

These studies considered the canonical problem of homogeneous and stratified plane Couette flow respectively, i.e. the flow of a viscous fluid between two plates being driven at a constant relative velocity, and when stratified, being maintained at a constant (stable) temperature difference, so that a constant density jump existed across the fluid layer. It is to be expected that the properties of the bounds on the dissipation and buoyancy flux are strongly dependent on the particular form of the flow forcing. Indeed, one particular type of forcing that commonly occurs is the application of stress $\tau = \rho u_\star^2$ (where $u_\star$ is the friction velocity) at the upper surface of a layer of fluid of depth h over a solid lower surface as happens, for example, when wind blows over a body of water. Tang, Caulfield & Young (2004) (henceforth TCY04) developed both upper and lower bounds for the mechanical energy dissipation rate for an unstratified fluid forced in this way. They found that the upper bound on the dissipation was given by $\varepsilon \leqslant \varepsilon_{\max} = u_\star^4/\nu$, i.e. the dissipation associated with the laminar linear velocity solution $\boldsymbol{u}_{\mathrm{L}} = \tau(z+h)/(\rho\nu)\hat{\boldsymbol{\imath}}$, where $\hat{\boldsymbol{\imath}}$ is the unit vector in the streamwise x-direction. The lower bound was shown to be $O(u_\star^3/h)$, independent to leading order of viscosity, as the Grashof number G, defined as $G = \tau h^2/(\rho\nu^2) = u_\star^2 h^2/\nu^2 \to \infty$. This lower bound is associated with a non-trivial flow velocity, such that the surface velocity has been substantially decelerated (when G is large) from the laminar value $u_{\mathrm{L}}(0) = u_\star^2 h/\nu = G^{1/2} u_\star$ to a value of order $u_\star \ll u_{\mathrm{L}}(0)$.

The aim of this paper is to identify bounds on the long-time average of the buoyancy flux of this flow. Since CTP04 demonstrated a close relationship between the stratified flows optimizing the buoyancy flux and the unstratified flows optimizing the dissipation in plane Couette flow, it is entirely plausible that the results of TCY04 will be relevant to this calculation. The rest of this paper is organized as follows. In § 2, I describe the model and the CDH method briefly, and in particular derive the functional which is optimized. In § 3, I show that this system can indeed be closely related to the system considered in TCY04, and so I derive rigorous bounds on the buoyancy flux directly, and discuss the properties of these results. Finally, in § 4, I draw some conclusions.

2. Model

As in TCY04, I consider an incompressible layer of fluid of constant depth h, variable temperature T, with kinematic viscosity ν, and thermal diffusivity κ. I assume that the density ρ of the fluid varies linearly with absolute temperature T. Following TCY04, I model the effect of the streamwise surface stress forcing $\tau\hat{\boldsymbol{\imath}}$ with a vertically varying body force, which typically will be chosen to be localized very close to the upper boundary. This model flow (referred to as flow B in TCY04) avoids the complexities of the treatment of boundary variations (see e.g. Courant & Hilbert 1953) while still allowing the study of surface-driven flow. As discussed in more detail in TCY04, provided the region over which the body force varies is always substantially shallower than (and embedded within) the characteristic depth of any surface boundary layer which develops in the bounding flow, this regularized model flow is equivalent mathematically to a purely surface-stress-driven flow. All calculations

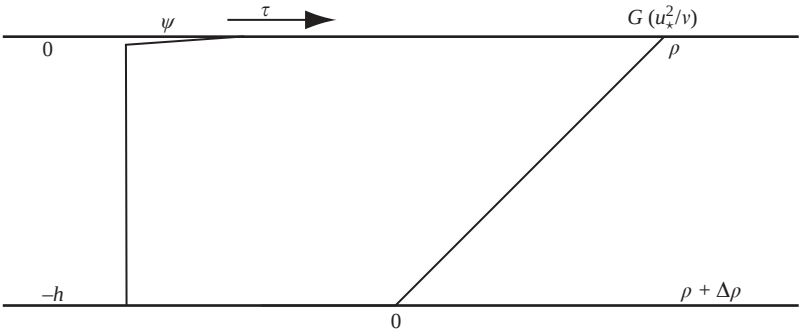

FIGURE 1. Schematic diagram showing the body-forced flow which, when the forcing profile function ψ only varies significantly from -1 in a thin region near $z=0$, is equivalent to a surface-stress-driven flow (see CTP04 for a fuller discussion, where this flow is referred to as flow B). The density boundary conditions and the laminar velocity profile (with surface velocity $u_\star^2/\nu$, or non-dimensionally G) are also shown.

were monitored to ensure that this embedding condition remained satisfied. I further assume that the constant total variation in density $\Delta\rho$ from $z=h$ to $z=0$ is sufficiently small compared to the surface density ρ_0 for the Boussinesq assumption to be valid. A schematic representation of the flow is shown in figure 1.

Therefore, the governing equations, non-dimensionalized with κ, h, ρ_0, and $\Delta\rho$, become

$$\boldsymbol{u}_t + \boldsymbol{u}\cdot\nabla\boldsymbol{u} + \nabla p - \sigma\nabla^2\boldsymbol{u} - \sigma^2 G\psi_z\hat{\boldsymbol{\imath}} + \sigma^2 GJ\hat{\boldsymbol{k}} = \boldsymbol{0}, \tag{2.1a}$$

$$\rho_t + \boldsymbol{u}\cdot\nabla\rho - \nabla^2\rho = 0, \tag{2.1b}$$

$$\nabla\cdot\boldsymbol{u} = 0, \tag{2.1c}$$

where the non-dimensional density ρ is the difference of the actual density from the (fixed surface) density scaled with the total density difference $\Delta\rho$. The appropriate boundary conditions are

$$\boldsymbol{u}(-1) = \boldsymbol{0}, \quad \rho(-1) = 1; \quad u_{1z}(0) = u_{2z}(0) = u_3(0) = \rho(0) = 0, \tag{2.2}$$

and in general, the behaviour of the system depends on three non-dimensional numbers, namely the Grashof number G, the (bulk) Richardson number J, and the Prandtl number σ, defined as

$$G = \frac{\tau h^2}{\rho\nu^2} = \frac{u_\star^2 h^2}{\nu^2}, \quad J = \frac{g\Delta\rho h}{\rho_0 u_\star^2}, \quad \sigma = \frac{\nu}{\kappa}, \tag{2.3}$$

defining in turn the friction velocity $u_\star$.

I impose a long-time-average and both x-periodic and y-periodic boundary conditions across $-L_x < x < L_x$, and $-L_y < y < L_y$ and so introduce a reasonable time and horizontal averaging operator:

$$\overline{q(\boldsymbol{x},t)} \equiv \lim_{T\to\infty}\frac{1}{4L_yL_xT}\int_0^T\int_{-L_y}^{L_y}\int_{-L_x}^{L_x} q(\boldsymbol{x},t)\,\mathrm{d}x\,\mathrm{d}y\,\mathrm{d}t\,; \quad q(\boldsymbol{x},t) = \overline{q}(z) + \hat{q}(\boldsymbol{x},t), \tag{2.4}$$

thus defining the meanless component $\hat{q}$ (such that $\overline{\hat{q}} = 0$) and a volume average:

$$\langle q(\boldsymbol{x},t)\rangle = \int_{-h}^{0}\overline{q}\,\mathrm{d}z\,. \tag{2.5}$$

The vertical distribution of the body force is captured by the profile function ψ, which is normalized so that $\langle\psi^2\rangle = 1$. Indeed, to model surface-driven motions, I choose $\psi \simeq -1$ over most of the depth of the fluid layer (and so there is little forcing) with sharp gradients in ψ (and hence forcing of $\boldsymbol{u}$) localized very close $z = 0$, where, to be consistent with the upper boundary condition on the velocity, $\psi(0) = 0$.

I wish to construct a bound on the long-time average of the buoyancy flux $\mathscr{B} = \sigma^2 GJ\langle u_3\rho\rangle$, or equivalently the variance of density fluctuations $\chi = \sigma^2 GJ\langle|\nabla\rho|^2\rangle$, since it is straightforward to establish that $\chi = \mathscr{B} + \sigma^2 GJ$. I use the CDH method, and so I decompose both the velocity and the density field into steady one-dimensional 'backgrounds' (which do not necessarily correspond to horizontally averaged means) with the same boundary conditions as the actual flow, and three-dimensional, unsteady fluctuations with homogeneous boundary conditions. Therefore, I postulate that

$$\boldsymbol{u}(\boldsymbol{x},t) = \phi(z)\hat{\boldsymbol{\imath}} + \boldsymbol{v}(\boldsymbol{x},t), \quad \rho(\boldsymbol{x},t) = \tau(z) + \theta(\boldsymbol{x},t), \tag{2.6}$$

$$\left.\begin{aligned} 0 = \phi(-1) = \theta(-1), \quad \tau(-1) = -1, \quad \boldsymbol{v}(-1) = \boldsymbol{0}, \\ 0 = \phi_z(0) = v_{1z}(0) = v_{2z}(0) = v_3(0) = \tau(0) = \theta(0) \end{aligned}\right\}. \tag{2.7}$$

As is well-known (and was mentioned in the introduction) a particular attraction of such a decomposition is that the background fields may be thought as fulfilling two roles: they act both as a representation of the actual bounding flow fields, and also as Lagrange multipliers to impose certain physically plausible constraints within a functional which can then be optimized, using conventional variational techniques, to obtain a rigorous bound on a flow quantity of interest. (See PK03 for more details) Since here we wish to construct a bound on the buoyancy flux, a natural functional to consider is

$$\begin{aligned} \mathscr{L} = {} & \sigma^2 GJ\langle|\nabla\rho|^2\rangle - a\langle\phi'(\overline{u_1u_3} - \sigma\overline{u}_1{}' - \sigma^2 G\psi)\rangle \\ & - a(\sigma\langle\|\nabla\boldsymbol{u}\|^2\rangle + \sigma^2 GJ\langle\rho u_3\rangle + G\sigma^2\langle\psi\overline{u}_1{}'\rangle) \\ & - b\sigma^2 GJ\left(\langle|\nabla\rho|^2\rangle + \tfrac{1}{2}\left[\overline{\rho}'\big|_0 + \overline{\rho}'\big|_1\right]\right) - b\sigma^2 GJ\langle\tau'(\overline{\rho u_3} - \overline{\rho}')\rangle, \end{aligned} \tag{2.8}$$

where $q' = \mathrm{d}q/\mathrm{d}z$, for purely z-dependent quantities $q(z)$. Written in this way, it is apparent that there are four Lagrange multipliers imposing four physical constraints: a which imposes total power balance, b which imposes entropy flux balance, $a\phi'$ which imposes horizontally averaged streamwise momentum balance, and $b\tau'$ which imposes horizontally averaged heat balance.

3. Results

Through considering the potential energy balance, it is straightforward to establish that $b = 2 - a$ in all cases where the buoyancy flux is non-zero. Then, a necessary condition for a particular set of $\boldsymbol{v}$, ϕ, θ, τ, and a to constitute a bounding solution is for the set to be a solution of the Euler–Lagrange equations obtained from taking variations of the functional $\mathscr{L}$ with respect to the members of this set. However, there is the possibility that there are several such solutions, and a further condition required to constitute an upper bound is that the solution satisfies a so-called spectral constraint (see for example PK03) which essentially demonstrates which solution to the Euler–Lagrange equations constitutes an upper bound.

A simple way to appreciate this issue is through consideration of the properties of the laminar solution:

$$\theta_{\mathrm{L}} = 0, \quad \boldsymbol{v}_{\mathrm{L}} = \boldsymbol{0}, \quad u_{1\mathrm{L}z} = \phi_{\mathrm{L}}' = -\sigma G\psi, \quad \rho_{\mathrm{L}z} = \tau_{\mathrm{L}}' = -1. \tag{3.1}$$

For all values of G with $a=1$ (and hence $b=1$) this solution satisfies the Euler–Lagrange equations, predicting a zero bound on the buoyancy flux, due to the absence of vertical velocity u_3. The spectral constraint for this flow is simply

$$\sigma\langle\|\nabla \boldsymbol{V}\|^2\rangle - \sigma G\langle\psi V_1 V_3\rangle \geqslant 0, \tag{3.2}$$

for all incompressible flow fields $\boldsymbol{V}$ which satisfy the homogeneous boundary conditions. This constraint clearly corresponds to the requirement that the flow is energy stable (see Joseph 1976) in the sense that all perturbations must decay monotonically with time. Therefore, the laminar flow with $a=1$ constitutes a bound provided that the flow is energy stable, which is true if $G \leqslant G_{es} = 51.7$ (see TCY04). For larger values of G, there exist non-trivial velocity fields $\boldsymbol{V}$ which violate the spectral constraint. However, analogously to the situation discussed in the context of stratified plane Couette flow (see CTP04) it is possible to identify a non-trivial solution to the full set of Euler–Lagrange equations with $a=1$ that still continues to satisfy the appropriate spectral constraint.

The fact that a bounding solution set can be shown to exist for the parameter $a=1$ has profound implications for the behaviour of the associated density field. Indeed, when $a=1$, the density field decouples from the velocity field, and is only required to satisfy

$$\tau' = -1, \quad \overline{\theta}' = \overline{\hat{v}_3\hat{\theta}} - \langle\hat{v}_3\hat{\theta}\rangle, \quad \sigma^2 GJ\langle\hat{v}_3\theta\rangle = \frac{\sigma}{4}\langle(\phi' + \sigma G\psi)^2\rangle. \tag{3.3}$$

In these expressions, the velocity fields are given as solutions of the Euler–Lagrange equations

$$2\bar{v}_1' + (\phi' + \sigma G\psi) = 0, \tag{3.4a}$$

$$2\overline{\hat{v}_1\hat{v}_3} - \sigma(\phi' + \sigma G\psi) = 0, \tag{3.4b}$$

$$2\sigma\nabla^2\hat{\boldsymbol{v}} - \phi'\begin{pmatrix}\hat{v}_3\\0\\\hat{v}_3\end{pmatrix} - \nabla\hat{p} = \boldsymbol{0}, \tag{3.4c}$$

where the perturbation pressure $\hat{p}$ imposes incompressibility on the meanless part $\hat{v}$, as defined by (2.4). For the solution set actually to constitute an (upper) bound, the so-determined ϕ (solution to (3.4)) must satisfy the spectral constraint, which takes the form

$$\langle\phi' V_1 V_3\rangle + \sigma\langle\|\nabla \boldsymbol{V}\|^2\rangle \geqslant 0, \tag{3.5}$$

for all incompressible $\boldsymbol{V}$ with homogeneous boundary conditions. For this solution set, from (3.3), the long-time-averaged buoyancy flux $\mathscr{B}$ is bounded by

$$\mathscr{B} \leqslant \mathscr{B}_{\max} = \frac{\sigma}{4}\langle(\phi' + \sigma G\psi)^2\rangle. \tag{3.6}$$

Construction of a solution set for these equations to arbitrary values of G can be simply achieved by noting that, under the transformations

$$\hat{\boldsymbol{v}} = \sigma\hat{\boldsymbol{v}}_\lambda, \quad \phi = \lambda\sigma\phi_\lambda, \quad G = (2-\lambda)G_\lambda, \tag{3.7a}$$

$$\lambda = \frac{\langle\|\nabla\hat{\boldsymbol{v}}_\lambda\|^2\rangle}{G_\lambda\langle\psi\hat{v}_{1\lambda}\hat{v}_{3\lambda}\rangle} = \frac{2\langle\|\nabla\hat{\boldsymbol{v}}\|^2\rangle}{G\langle\psi\hat{v}_1\hat{v}_3\rangle + \langle\|\nabla\hat{\boldsymbol{v}}\|^2\rangle}, \tag{3.7b}$$

the Euler–Lagrange equations (3.4*b*) and (3.4*c*) determining ϕ and $\hat{\boldsymbol{v}}$, and the spectral constraint (3.5) correspond to those used in TCY04 to generate a lower bound $\mathscr{E}_{\min}$ on

the mechanical energy dissipation rate in an identically forced flow. In that problem, the parameter λ is determined from (3.7*b*) as part of a solution set including $\hat{\boldsymbol{v}}_\lambda$ and ϕ_λ. Here, on the other hand, for the problem of maximizing the long-time average of the buoyancy flux, once a given solution $\hat{\boldsymbol{v}}_\lambda$, ϕ_λ and λ is identified at G_λ from the mechanical energy dissipation rate problem, the appropriate corresponding value for G for the buoyancy flux problem is determined using this value of λ in (3.7*a*).

Since, as discussed in TCY04, $\lambda = 1$ at the energy stability point, $G = G_{es} = G_\lambda$ there. However, as G_λ increases, λ decreases, though it still remains positive, a fact which can also be established from (3.7*b*), since

$$\sigma G \langle \psi \hat{v}_1 \hat{v}_3 \rangle = \sigma \langle \|\boldsymbol{\nabla} \hat{\boldsymbol{v}}\|^2 \rangle + 2\mathscr{B}. \tag{3.8}$$

Therefore, the required solution set $\phi, \hat{\boldsymbol{v}}$ for the upper bound for the long-time-averaged buoyancy flux at a particular G corresponds to the solution set $\phi_\lambda, \hat{\boldsymbol{v}}_\lambda$ for the lower bound on the dissipation at a typically smaller value G_λ of the Grashof number. Using this solution set, it is then possible to construct the upper bound on the long-time-averaged buoyancy flux from the previous result presented in TCY04 without further calculation, if it is once again assumed that streamwise variations can be ignored.

From (3.6), using the transformations (3.7*a*), the bound corresponds to

$$\mathscr{B} \leqslant \mathscr{B}_{\max} = (1-\lambda)\sigma^3 \left[\frac{G^2}{(2-\lambda)^2} - \mathscr{E}_{\min}|_{G/(2-\lambda)} \right]. \tag{3.9}$$

For the particular form of the forcing profile function ψ considered in TCY04 (where $\psi(z)$ was labelled $\sigma(z)$) with $\psi \simeq -1$ over all but a vanishingly small layer (always verified to be significantly smaller than any boundary layers which develop: see TCY04 for details) near the upper interface at $h = 0$ where $\psi \to 0$ (thus mimicking a surface-stress-driven flow), $\mathscr{E}_{\min}$ was calculated numerically using the method originally described in PK03, which is based upon the numerical continuation package PITCON (Rheinboldt & Burkhardt 1983*a*, *b*). The calculated bound for such a profile function ψ is

$$\mathscr{E}|_{G_\lambda} \geqslant \mathscr{E}_{\min}|_{G_\lambda} = 7.531 G_\lambda^{3/2} - 20.3 G_\lambda + O\left(G_\lambda^{1/2}\right), \tag{3.10}$$

while as $G_\lambda \to \infty$, $\lambda = O(G_\lambda^{-1/2})$, thus implying that, to leading order, as $G \to \infty$

$$\mathscr{B} \leqslant \mathscr{B}_{\max} = \sigma^3 \frac{G^2}{4} + O\left(G^{3/2}\right). \tag{3.11}$$

The actual bound for all calculated G is shown in figure 2(*a*). For simplicity, the Prandtl number σ is set to one.

Dimensionally, this implies that the long-time-averaged upper bound on the dimensional buoyancy flux $\mathscr{B}^* \leqslant \mathscr{B}^*_{\max}$ is

$$\mathscr{B}^* \leqslant \mathscr{B}^*_{\max} = \frac{\kappa^3}{h^4} \mathscr{B}_{\max} = \frac{u_\star^4}{4\nu} + O\left(\frac{u_\star^3}{h}\right), \tag{3.12}$$

using the friction velocity as defined in (2.3).

This bounding scaling involves the fluid kinematic viscosity, yet is independent of the flow depth. These characteristics can best be understood by considering the flow velocity fields which determine this bound, since the density field is determined completely by the velocities. A first natural step is to consider the long-time-averaged

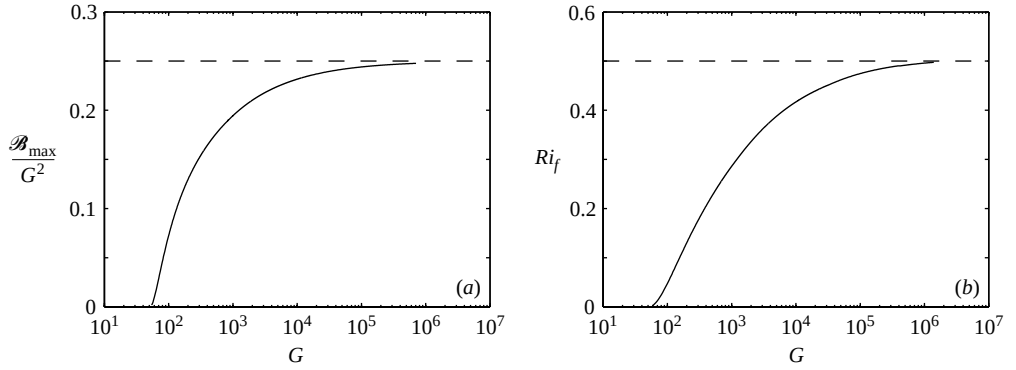

FIGURE 2. Plots against Grashof number of: (*a*) the upper bound on the long-time-averaged buoyancy flux scaled with the square of the Grashof number i.e. $\mathscr{B}_{\max}/G^2$; (*b*) the associated value of the flux Richardson number Ri_f as defined in (3.18). For simplicity the Prandtl number $\sigma = 1$.

mechanical energy dissipation rate $\mathscr{E}$, defined non-dimensionally as

$$\mathscr{E} \equiv \sigma \langle \|\nabla \boldsymbol{u}\|^2 \rangle = \sigma \langle (\phi' + \overline{v_1}')^2 \rangle + \sigma \langle \|\nabla \hat{\boldsymbol{v}}\|^2 \rangle = \overline{\mathscr{E}} + \hat{\mathscr{E}}, \tag{3.13}$$

for the velocity fields which determine the upper bound on the buoyancy flux.

Using (3.4*a*), (3.4*b*), (3.6), (3.7*b*) and (3.8), it is possible to show that

$$\hat{\mathscr{E}}_{\max} = \left(\frac{\lambda}{1-\lambda}\right)\mathscr{B}_{\max}, \quad \overline{\mathscr{E}}_{\max} = \sigma^3 G^2 + \left(\frac{\lambda - 3}{1-\lambda}\right)\mathscr{B}_{\max}, \tag{3.14}$$

where the subscript 'max' denotes using the velocity fields associated with the upper bound on the buoyancy flux, and so

$$\mathscr{E}_{\max} = \sigma^3 G^2 - \left(\frac{3-2\lambda}{1-\lambda}\right)\mathscr{B}_{\max} \to \frac{\sigma^3 G^2}{4} + O\left(\sigma^3 G^{3/2}\right), \tag{3.15}$$

as $G \to \infty$. This associated dissipation is substantially larger than the lower bound identified in TCY04, which is $O(\sigma^3 G^{3/2})$ within the non-dimensionalization used in this paper, and indeed it has the scaling (though not the numerical factor) associated with the upper bound derived in TCY04 corresponding to a laminar velocity profile driven by the surface forcing, which corresponds to

$$\mathscr{E}_{\mathrm{L}} = \sigma^3 G^2; \quad \mathscr{E}^*_{\mathrm{L}} = \frac{u_\star^4}{\nu}. \tag{3.16}$$

As is apparent from (3.7*a*), since $\lambda = O(G^{-1/2})$ as $G \to \infty$, $\phi \ll \phi_\lambda$ at large G. This is a major, qualitative difference between the two problems. For both problems, the background velocity field has the same structure, with boundary layers of depth of order $O(G^{-1/2})$ where, for this problem, $\phi' = O(\sigma G)$, with $\phi' \approx 0$ in the interior of the fluid layer, as is shown in figure 3(*a*). Such a structure of course is enforcing the horizontally averaged streamwise momentum constraint, with the boundary forcing being balanced by the Reynolds stress. However, whereas in the unstratified problem, the gradient of the mean velocity profile in the interior of the flow domain is $O(\sigma G^{1/2})$, rising to $O(\sigma G)$ only within the boundary layers, since $\overline{u_1}' = \phi' + \overline{v_1}'$ by definition, (3.4*a*) and (3.7*a*) imply that, for the stratified problem,

$$\overline{u_1}' = \tfrac{1}{2}(\phi' - \sigma G \psi) \simeq \frac{\sigma G}{2} \simeq \sigma G_\lambda \text{ as } G \to \infty. \tag{3.17}$$

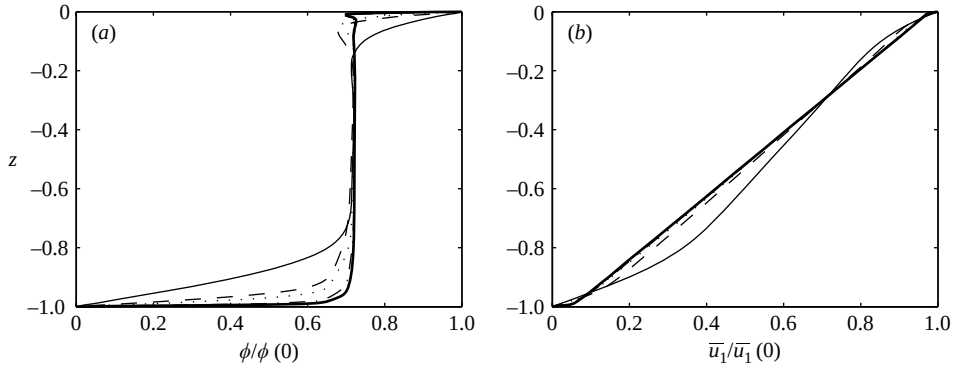

FIGURE 3. Vertical profiles of (*a*) $\phi/\phi(0)$ and (*b*) $\overline{u_1}/\overline{u_1}(0)$ associated with an upper bound on the buoyancy flux for: $G = 1065$ (plotted with a thin solid line); $G = 10108$ (dashed line); $G = 23798$ (dotted line); $G = 172097$ (dot-dashed line); $G = 462577$ (thick solid line). For these choices, $\overline{u_1}(0)/\phi(0) = 1.6186$, 3.7497, 5.4384, 6.1211 and 6.8485 respectively, which ratio is $O(G^{1/2})$ as $G \to \infty$ as expected.

Therefore, to leading order at least, the mean velocity profile associated with the upper bound in the long-time-averaged buoyancy flux corresponds to a mean laminar velocity profile at smaller (by a factor of two) Grashof number. The contribution to the dissipation from the horizontally averaged flow $\overline{\mathscr{E}}_{\max}$ completely dominates the dissipation at large G, since (3.14) implies that $\hat{\mathscr{E}}_{\max} = O(\lambda \mathscr{B}_{\max}) = O(\sigma^3 G^{3/2})$ as $G \to \infty$. Also, since the background profile ϕ becomes insignificant to leading order, the mean velocity profile does not exhibit the strong boundary layer structure characteristic of ϕ discussed in TCY04, and the mean velocity profile is essentially laminar, with the same qualitative constant-gradient linear structure as a laminar flow. In figure 3, we illustrate this fact by plotting characteristic vertical profiles of both $\phi/\phi(0)$ and $\overline{u_1}/\overline{u_1}(0)$ for flows with various G. It is apparent that the evident boundary layers in the structure of ϕ have little influence on the structure of $\overline{u_1}$, particularly as G approaches large values.

Clearly, the laminarity of the mean flow dominates and makes the dissipation large compared to the lower bound scaling for an unstratified flow. This is due fundamentally to the fact that the surface velocity is largest for the laminar flow, being essentially σG_λ for any G_λ, and thus allowing the largest overall possible values for velocity gradients throughout the flow. Such high-speed surface flows similarly lead to the largest possible gradients in density variations, and hence to maximization of the flow buoyancy flux. However, since the energy input by the surface forcing is balanced not only by the viscous dissipation, but also by the buoyancy flux, there appears to be a necessity for some deceleration (by a factor of two) of the surface velocity from its maximum possible value, since as $G \to \infty$, $\overline{u_1}(0) \to \sigma G/2$.

In essence, the upper bound on the buoyancy flux appears to coincide with a flow that is, in some sense, 'pseudo-laminar', with a scaling characteristic of a laminar velocity profile. This has implications for the flux Richardson number Ri_f, or equivalently the mixing efficiency of the flow η, defined, for the bounding solutions, as

$$\eta = Ri_f \equiv \frac{\mathscr{B}_{\max}}{\mathscr{B}_{\max} + \mathscr{E}_{\max}} = \frac{(1-\lambda)\mathscr{B}_{\max}}{(1-\lambda)\sigma^3 G^2 - (2-\lambda)\mathscr{B}_{\max}}, \tag{3.18}$$

upon substituting the appropriate value for the dissipation associated with the upper bound for the buoyancy flux, as defined in (3.11). Defined in this way, the

flux Richardson number quantifies the proportion of the energy input into the flow that leads to long-time-averaged buoyancy flux, and hence irreversible mixing. Asymptotically, using (3.11), $Ri_f \to 1/2$ as $G \to \infty$, implying an equipartition between the energy from the forcing which is lost to viscous dissipation and the energy which is lost to buoyancy flux (and hence the potential energy reservoir). This quantity is plotted in figure 2(*b*) for all G.

Furthermore, although, just as in CTP04, the detailed structure of the density profile cannot be determined explicitly due to the degeneracy in the Euler–Lagrange equations for the density field, certain aspects of the spatial localization of the mixing can be inferred from (3.3), (3.4*a*) and (3.4*b*). At the lower boundary, these equations imply that

$$\sigma^2 G J \overline{\theta}'\big|_{z=-1} = -\mathscr{B}_{\max}; \quad \overline{u_1}'\big|_{z=-1} = -\sigma G \psi. \tag{3.19}$$

The appropriate measure of the relative importance of the stratification and shear is the gradient Richardson number $Ri(z)$, defined as

$$Ri(z) = -\sigma^2 G J \frac{\mathrm{d}\overline{\rho}}{\mathrm{d}z}\left(\frac{\mathrm{d}\overline{u}_1}{\mathrm{d}z}\right)^{-2}. \tag{3.20}$$

Therefore, at the lower boundary, as $G \to \infty$

$$Ri(-1) = \frac{\mathscr{B}_{\max} + \sigma^2 G J}{\sigma^2 G^2 \psi^2} \simeq \frac{\sigma}{4}, \tag{3.21}$$

and so locally the stratification remains significant. This is principally due to the fact (as already noted) that the velocity field does not develop strong boundary layers, and so the shear is not increased markedly near $z = -1$. Furthermore, from (3.3), the magnitude of the gradient in $\overline{\theta}$ must decrease towards the interior of the flow, while the velocity shear remains approximately constant. Therefore, $Ri(z)$ is likely to be substantially less in the interior of the flow. This implies that the mixing is likely to be dominated by mixing in the interior of the flow, rather than at the boundaries, which is a major qualitative difference between this flow and the stratified Couette flow discussed in CTP04.

4. Conclusions

Using the CDH method, I have generated a bound on the long-time average of the bouyancy flux within a surface-driven flow. Just as in plane Couette flow (considered in CTP04) the bound is associated with a decoupling of the density fields from the velocity fields in the Euler–Lagrange equations of the variational problem. This leads to a close relationship between the meanless fluctuation and background fields associated with the buoyancy flux bound and the equivalent fields determined for identifying bounds on dissipation in an unstratified flow (as discussed in more detail in WCP04).

However, this analogous decoupling actually leads to a qualitative difference between the properties of the bounds for stratified plane Couette flow and the surface-driven flow discussed in this paper. For surface-driven flow, the characteristic scaling for the upper bound on the long-time average of the buoyancy flux is that of a laminar flow as it is $O(u_\star^4/\nu)$, dependent on the viscosity of the fluid, but independent of the layer depth. The associated velocity profile is linear, with a dimensional surface velocity of $u_\star^2/(2\nu)$ to leading order. This deceleration from the purely laminar unstratified velocity profile (with surface velocity $u_\star^2/\nu$) is due to the surface forcing

also feeding energy into the potential energy reservoir through the buoyancy flux, and hence mixing. Although the associated density distribution is not uniquely specified, by consideration of the properties of the gradient Richardson number at the lower boundary of the flow, it is apparent that significant mixing is to be expected in the interior of the flow domain.

This pseudo-laminarity in the bounding flows at least suggests the possibility of high levels of very efficient mixing within such flows. This suggestion is consistent with direct numerical simulations of transitional shear flows, where, at least under some circumstances, Smyth, Moum & Caldwell (2001) observed that significant amounts of mixing could occur during the 'pre-turbulent' phase of flow evolution, when the dissipation and buoyancy flux within the flow exhibit laminar-like scaling properties. It also is a possible explanation for the observations of anomalously high mixing efficiency (of the order of $Ri_f \sim 1/2$) observed in the stratified interior of Lake Baikal (see figure 4*e* of Ravens *et al.* 2000) where wind forcing appears to be an important driving mechanism. However, as is a common concern with bounding calculations such as are presented here, it remains to be seen how closely real flows approach the predicted bound (which can naturally be investigated using direct numerical simulation) and also whether there are further appropriate physically plausible constraints which should be applied to improve the quality and usefulness of the calculated bounds.

I would like to thank W. Tang for kindly sharing his numerical data, and also the National Science Foundation for support under the Collaborations in Mathematical Geosciences (CMG) initiative (ATM-0222104).

REFERENCES

Caulfield, C. P., Tang, W. & Plasting, S. C. 2004 Reynolds number dependence of an upper bound for the long-time averaged buoyancy flux in plane stratified Couette flow. *J. Fluid Mech.* **498**, 315–332 (referred to herein as CTP04).

Courant, R. & Hilbert, D. 1953 *Methods of Mathematical Physics,* Vol. 1, 1st English Edn. Interscience.

Doering, C. R. & Constantin, P. 1992 Energy dissipation in shear driven turbulence. *Phys. Rev. Lett.* **69**, 1648–1651.

Hopf, E. 1941 Ein allgemeiner endlichkeitssatz der hydrodynamik. *Mathematische Annalen* **117**, 764–775.

Joseph, D. D. 1976 *Stability of Fluid Motions I.* Springer.

Nicodemus, R., Grossmann, S. & Holthaus, M. 1997 Improved variational principle for bounds on energy dissipation in turbulent shear flow. *Physica* D **101**, 178–190.

Plasting, S. C. & Kerswell, R. R. 2003 Improved upper bound on the energy dissipation rate in plane Couette flow: The full solution to Busse's problem and the Constantin-Doering-Hopf problem with 1-D background field. *J. Fluid Mech.* **477**, 363–379 (referred to herein as PK03).

Ravens, T. M., Kocsis, O., Wuest, A. & Granin, N. 2000 Small-scale turbulence and vertical mixing in Lake Baikal. *Limnol. Oceanogr.* **45**, 159–173.

Rheinboldt, W. C. & Burkhardt, J. V. 1983*a* ALGORITHM 596 a program for a locally parameterized continuation process. *ACM Trans. Math. Software* **9**, 236–241.

Rheinboldt, W. C. & Burkhardt, J. V. 1983*b* A locally parameterized continuation process. *ACM Trans. Math. Software* **9**, 215–235.

Smyth, W. D., Moum, J. N. & Caldwell, D. R. 2001 The efficiency of mixing in turbulent patches: inferences from direct simulations and microstructure observations. *J. Phys. Oceanogr.* **31**, 1969–1992.

Tang, W., Caulfield, C. P. & Young, W. R. 2004 Bounds on dissipation in stress-driven flow. *J. Fluid Mech.* **510**, 333–352 (referred to herein as TCY04).